COBEM 2023 27TH INTERNATIONAL CONGRESS OF MECHANICAL ENGINEERING

ABCM Brazilian Society of Mechanical Sciences and Engineering
27th ABCM International Congress of Mechanical Engineering
December 04-08, 2023, Florianópolis-SC, Brazil

COB-2023-1222

Predicting of Temperatures Profiles Along an Earth-Air Heat Exchanger (EAHE) Using Artificial Neural Networks

Leonardo Bruno Foltran
Hugo Valadares Siqueira
Gerson Henrique dos Santos
Victor Vaurek Dimbarre
Thiago Antonini Alves
Federal University of Technology – Paraná.
Rua Dr Washington Subtil Chueire, 330, 84017-220, Ponta Grossa, PR, Brazil.

Abstract. *In Brazil, buildings account for proximately 51% of electricity consumption. In commercial buildings, air conditioning systems are responsible for about 70% of this use. To collaborate to reduce this demand, this work presents an Earth-Air Heat Exchanger (EAHE) used for environment climatization. This passive system uses the soil as a heat exchanger, heating or cooling the air depending on the climatic conditions. The system, which includes 100 mm diameter Polyvinyl Chloride (PVC) ducts, and a fan for airflow control, was built at the Federal University of Technology of Paraná (UTFPR), Campus Ponta Grossa. A series of k-type thermocouples were inserted along the EAHE, the ground, and the environment. Artificial Neural Networks (ANNs) were used to obtain the temperature distribution along the exchanger to predict the performance of these heat exchangers subjected to different climatic conditions. Air temperature at the exchanger inlet, soil temperature, and airflow rate were used as input data for the model. Four different structures of Multilayer Perceptron (MLP) networks were used in this study, and all of them were capable of adequately predicting the temperatures of the thermocouples along the heat exchanger.*
Keywords: *Earth-Air Heat Exchangers (EAHE), Energy Efficiency, Passive Cooling, Artificial Neural Networks (ANNs), Multilayer Perceptron (MLP).*

1. Introduction

In Brazil, half of the energy consumed in recent decades came from buildings, which grew proportionally to the Gross Domestic Product (GDP). In this context, research on the energy efficiency of buildings has grown in developing countries, primarily when related to finite resources in nature. Intending to evolve this scenario, reducing the energy demand necessary for thermal control in buildings, it proved to be very promising. In this way, the literature offers several alternatives (Brugnera et al., 2019). Among them, one of the alternatives highlighted to reduce energy consumption and improve comfort conditions in buildings is using soil as a heat exchanger. Due to its high thermal inertia, the soil can maintain an almost constant temperature at specific depths, with little dependence on temperature variations that occur on the surface (Marcondes et al., 2010; Ramírez-Dávila et al., 2014; Hollmuler et al., 2014; Rodrigues et al., 2017). In this case, the Earth-Air Heat Exchanger (EAHE) uses the soil to heat or cool the air through buried ducts, usually made of polyvinyl chloride (PVC). The EAHE can operate in different ways, such as capturing external air (open system), circulating the air from the internal environment (closed system), or in a hybrid way, taking advantage of the internal air and adding a portion of external air (Soni et al., 2015; Bordoloi et al., 2018).

In addition to the high computational time required, analyzing the performance of EAHE through numerical simulations can be complex due to the nonlinear interactions among various variables, including air temperature, humidity, airflow, and soil characteristics. Therefore, accurately predicting the temperature distribution along the exchanger pipe requires the appropriate modeling of these complex interactions. Artificial neural networks (ANNs), such as the multilayer perceptron (MPL) architecture, can be appropriate for carrying out these predictions, as Haykin (2009) discusses in his book "Neural Networks and Learning Machines". By training an MLP, using historical operational data from the heat exchanger, we can estimate temperature variations along the tube, even under different initial physical conditions, such as varying airflow rates, soil temperatures, and atmospheric air temperatures. The use of this model enables optimizing the operation of the heat exchanger, predicting the temperature distribution throughout the system and, consequently, becoming possible to improve energy efficiency and performance.

Results from studies that have analyzed the performance of ANNs in heat exchangers demonstrate that properly trained neural networks can simulate both the general and specific characteristics of a heat exchanger (Tan et al., 2009). For example, in an article published by Romero-Méndez et al. (2016), it is revealed the convenience of using neural networks as a precise prediction tool for determining convective heat transfer rates in evaporators. Additionally, Kumar et al. (2006) describe that for a EAHE, the use of an algorithm is suitable for calculating the outlet air temperature, as

well as the heating and cooling potential of the system. Moreover, the use of ANNs for time series prediction is highly appropriate, as evidenced by Siqueira et al. (2020), where the utilization of extreme machine learning (EML) neural network demonstrated satisfactory performance for this type of forecasting.

As observed in the literature, the use of ANNs to analyze the performance of heat exchangers, in general, has yet to be explored, especially concerning the EAHE. Thus, in this work, ANNs were used to obtain the temperature distribution along the exchanger to predict the performance of these heat exchangers subjected to different climatic conditions. The models were validated using data obtained experimentally through a prototype built at the Federal Technological University of Paraná (UTFPR), Campus Ponta Grossa, Brazil.

2. Experimental procedure

The experimental setup was developed at the Federal Technological University - Paraná (UTFPR), Campus Ponta Grossa. Figure 1(a) show the exchanger design and Figure 1(b) the location where it was installed, as well as their respective dimensions:

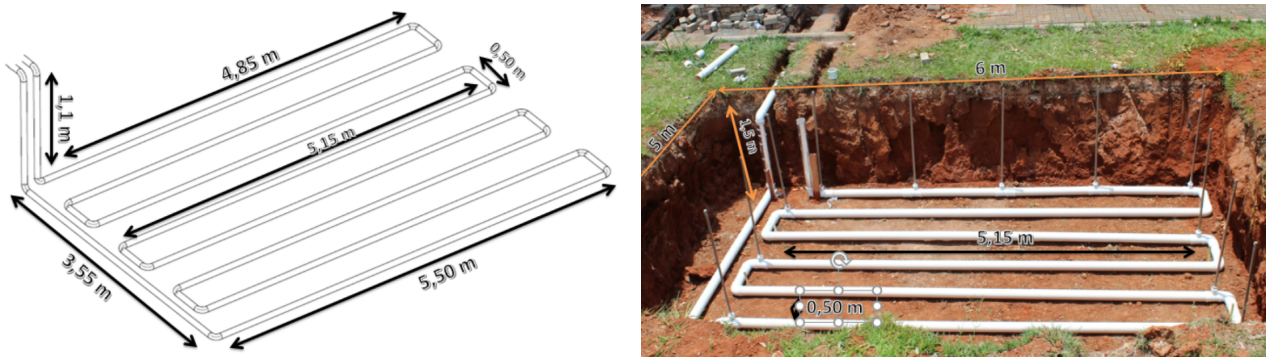

(a) (b)

Figure 1. (a) Design, (b) Mounting location.

Assembled with 100 mm diameter polyvinyl chloride (PVC) tubes in the form of serpentine and buried at a depth of 1.5 m from the surface, the EAHE has tubes with an average length of 5.15 m and spacing of 0.50 m between them, totaling 50.65 m in length. In the system, the air is insufflated by an AeroMack radial fan, model cre-03, with a power of 2 HP and a maximum flow of 3.2 m³/min. It should be noted that a much lower fan power would be sufficient for system operation. For this research, three different air flow velocities were analyzed: 3 m/s, 5 m/s, and 7.5 m/s, which were measured using a digital anemometer during operation.

14 K-type thermocouples were installed along the pipeline for temperature measurement, as shown in Figure 2(a). The first five are positioned in the first 4.85 meters (first pass), and the others every 5.60 meters of pipe. Figure 2(b) shows the apparatus for data acquisition composed of a Keysight™ DAQ970 data acquisition system (A), two Keysight™ multiplexers (B), and an Intel™ Core i7-7600 microcomputer with 16 GB of RAM (C).

(a) (b)

Figure 2. (a) Installation of thermocouples, (b) Data acquisition apparatus.

3. Multilayer perceptron

MLPs are networks capable of learning complex non-linear patterns between input and output variables, making them adequate for classification, regression and other tasks. These networks consist of multiple layers of interconnected

neurons, which are divided into an input layer, one or more intermediate (or hidden) layers, and an output layer (Haykin, 2009), as presented in Figure 3.

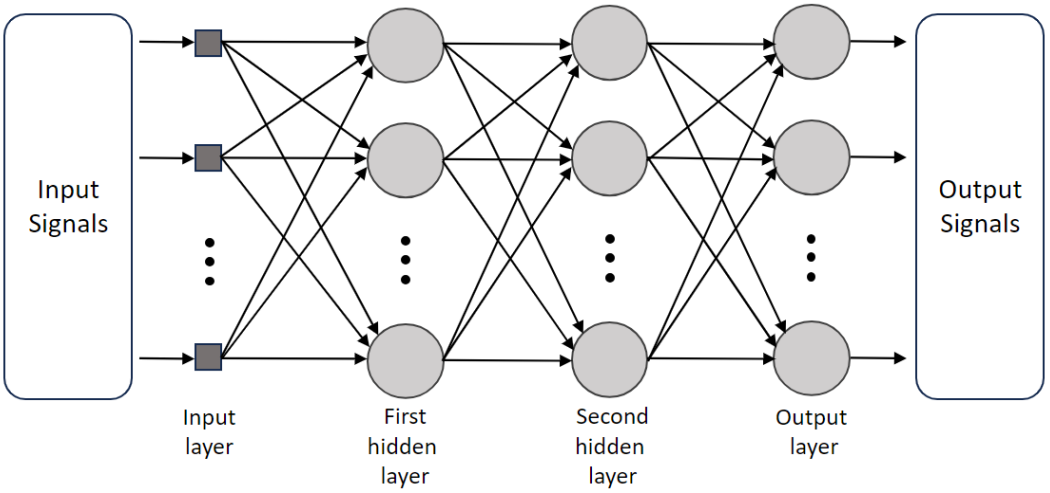

Figure 3. Representation of a multilayer perceptron structure with two hidden layers.

Each neuron in a hidden layer receives input signals from the previous layer, where they are weighted by the synaptic weights associated with each connection, which determine how much each input signal contributes to the neuron's output (Haykin, 2009). The weighted sum of the input signals is then passed through the neuron's activation function, which introduces non-linearities to the neuron's outputs. Mathematically, the output of each neuron can be expressed by the Eq. (1):

$$y = f(\sum_{i=1}^{n} w_i \cdot x_i + b), \tag{1}$$

where y represents the output of the neuron, f denotes the activation function, w_i represents the weights associated with each input x_i, b is the bias term, and n is the number of inputs to the neuron.

If there are more than one hidden layer, this process is repeated until the signal reaches the output layer. The output layer of the MLP has neurons that process the signals received from the hidden layers, apply a specific activation function, and combine these signals to produce the final output result of the network (Haykin, 2009).

After this process, the phase called backpropagation begins. In this phase, the error between the network's output and the desired value is propagated back to the previous layers. The synaptic weights of each neuron are updated according to the gradient descent, which calculates the direction and magnitude of the necessary adjustment to reduce the error. This process is iteratively repeated to adjust the weights in all layers, gradually improving the network's learning (Silva et al., 2010).

4. MLP APPLICATION

4.1 Data processing

Initially, the data was separated into input and output sets. The input data consisted of the following variables: air velocity in the pipeline, soil temperature, and air temperature at the inlet of the heat exchanger (first thermocouple). On the other hand, the output data was composed of temperatures recorded by the other 13 thermocouples along the pipeline. The output data were used to compare the predicted results by the networks, allowing for the evaluation of the network's performance and improvement of its training.

Before training the network, all the data used was normalized using the Min-Max method. Min-Max normalization ensures that all variable values are on the same scale, preventing values of larger magnitudes from dominating the learning process, in addition, it also improves the convergence speed of the optimization algorithm. The equation below expresses the method mathematically:

$$z_{norm} = (z - z_{min})/(z_{max} + z_{min}), \tag{2}$$

where z is the original value of the variable, z_{norm} is the normalized value of the variable, z_{min} and z_{max} are the minimum and maximum values of the variable, respectively.

After this step, it is essential to divide all dataset (input and output data) into three parts: training, validation, and test sets. The training set is used to adjust the network's weights and minimize the error during the learning process. In this study, 80% of the collected data was allocated to the training set, while the remaining 20% was assigned to the test set.

The validation set is a separate portion of the training data used to validate the model. In this case, 20% of the training set was dedicated to validation. For this research, the Early Stop validation method was employed. This technique is suitable for improving the efficiency and generalization capability of the model by preventing overfitting, a phenomenon that occurs when the model excessively adapts to the training data, resulting in poor performance during the test phase.

Finally, the test set is used to evaluate the final performance of the model. It measures how well the model performs on unseen data after training and validation phases.

4.2 The network structure

To facilitate the search in finding the best prediction results, it is interesting to explore different MLP network structures, as some structures may be more suitable for capturing the complex patterns and relationships present in the data than others.

For this research, four distinct types of structures were analyzed for comparison purposes, as described in Table 1.

Table 1. MLPs structures used for training.

Model number	Model structure	Input data	Hidden layers	Node numbers (per hidden layer)	Activation function (per hidden layer)	Optimization Algorithm	Output data	Validation loss
1	MLP	Air flow rate; soil temperature; atmospheric temperature.	2	20; 20	Sigmoid; Sigmoid	Adam	12 sensors	MSE
2			2	20; 20	Tanh; Tanh		12 sensors	
3			1	15	Sigmoid		1 sensor	
4			1	15	Tanh		1 sensor	

For models 1 and 2, the networks have 12 outputs, each one corresponding to the thermocouples installed along the exchanger's pipeline. For models 3 and 4, the networks have only 1 output, corresponding to a single thermocouple sensor, in other words, the network was trained 12 times, once for each sensor.

In this research, to optimize the search for the ideal set of weights that leads to optimal network performance, among the various existing optimization algorithms, Adam was chosen. The Adam algorithm combines the advantages of the stochastic gradient descent (SGD) method with the adaptive learning rate method, improving the efficiency and convergence speed of model training (Kingma and Ba, 2014).

For the purpose of comparison, the differences between models 1 and 2, as well as between 3 and 4, stem from the activation functions used. Specifically, models 1 and 3 employed the sigmoid function, represented by Eq. (3), while models 2 and 4 utilized the hyperbolic tangent function, represented by Eq. (4):

$$f(x) = (1 + exp(-x))^{-1}, \tag{3}$$

$$f(x) = (exp(x) - exp(-x))/(exp(x) + exp(-x)). \tag{4}$$

The loss calculated during the validation phase of the training (validation loss) was based on the mean squared error (MSE). MSE is a common metric used to evaluate the performance of regression models and can be expressed by Eq. 5:

$$MSE = (\Sigma(v - \overline{v})^2)/n, \tag{5}$$

where n is the total number of samples in the evaluation data, v represents the real or observed values and $\overline{v}$ represents the predicted or estimated values by the model.

In order to compare the performance of the networks' results, in addition to the MSE metric, the mean absolute error (MAE) metric and the maximum temperature error (MTE) were also utilized, both defined as:

$$MAE = (\Sigma|v - \overline{v}|)/n, \tag{6}$$

$$MTE = max(\left|v_{predicted} - v_{real}\right|), \tag{7}$$

where $max()$ is a function that returns the highest value obtained from the difference between each pair of predicted value ($v_{predicted}$) and real value (v_{real}) across all the analyzed data.

It is important to highlight that the four MLP models were subjected to independent training for 30 times. Each training was initiated with different random parameters, allowing the models to explore different learning trajectories and avoid getting stuck in local minima, which enables obtaining a more accurate and representative view of each model's behavior regarding the data and the variability of the obtained results.

5. Results

Based on the data collected from the thermocouple sensors and the digital anemometer, during the period from November and December 2021, January, February, and from May to December 2022, and from February to June 2023, with data collected hourly, resulting in a total of 19,470 data points (with each data point containing the output signals from the thermocouples and digital anemometers), the training results for the four MLP models can be observed in Table 2 below.

Table 2. Comparison of MSE, MAE e MTE for all MLPs models.

Model number	MSE	MAE	MTE (°C)
1	0.0078	0.0634	0.67
2	0.0063	0.0568	0.62
3	0.0115	0.0774	0.70
4	0.0103	0.0726	0.67

To better compare the test results, the box plot (Figure 4) illustrates the distribution of the MSE from all the conducted trainings for each model.

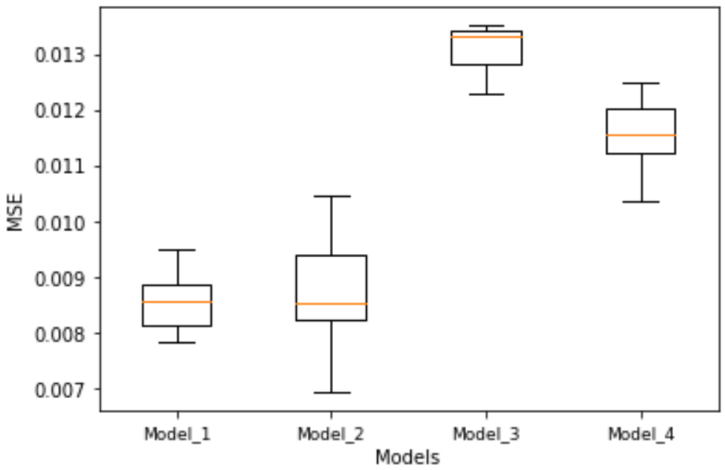

Figure 4. Boxplot of MSE for each model.

The scatter plots (Figure 5) below compare the predicted values with the true values for the test set, based on the best-performing MLP for each model.

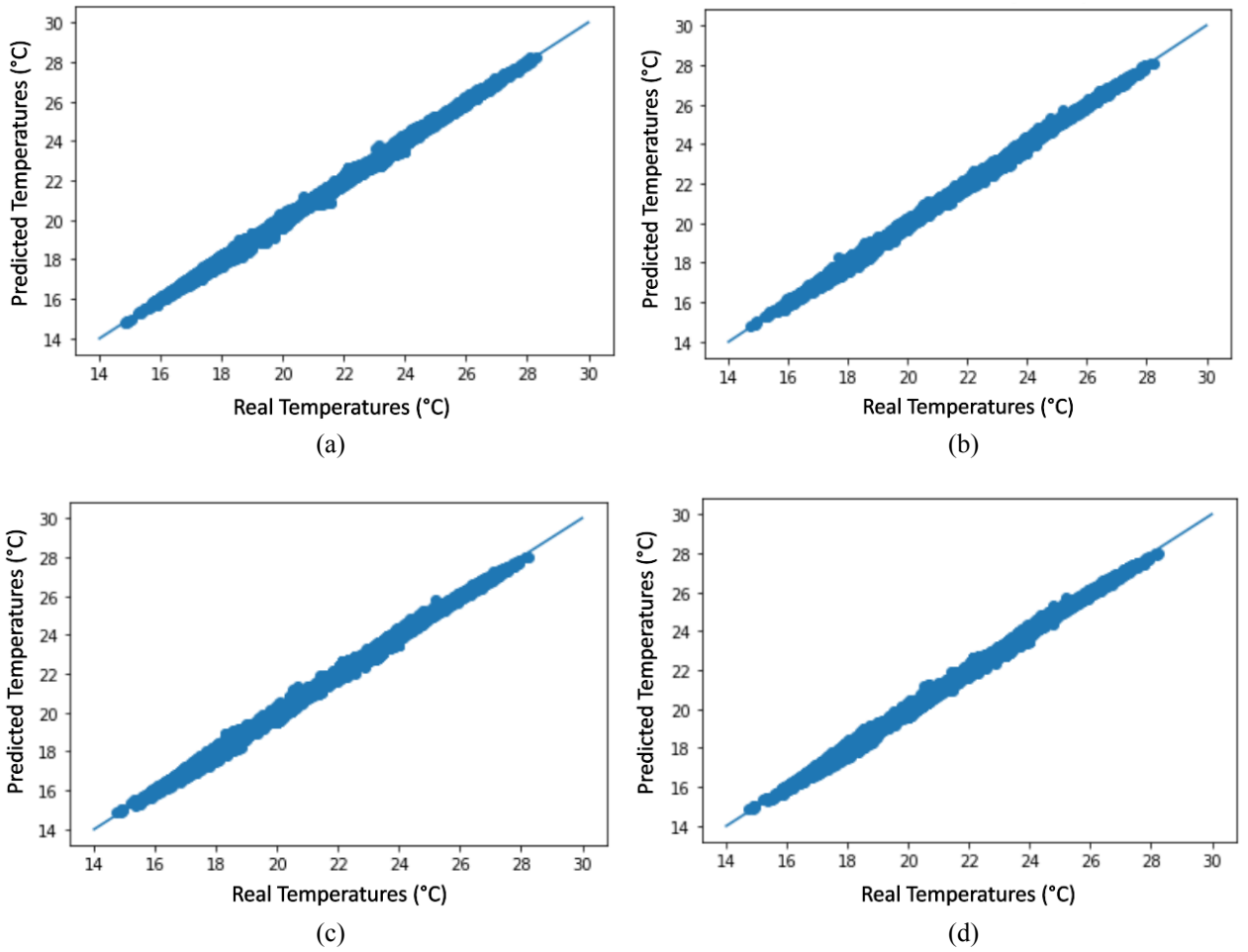

Figure 5. Comparison of predicted and real temperatures values for MLPs: (a) Model 1, (b) Model 2, (c) Model 3, (d) Model 4.

Based on the data from Table 2, it can be stated that the best model (among the structures listed in Table 1) was Model 2, as it exhibited the lowest MSE, MAE, and MTE values. Although, it is also noteworthy that Model 2 shows a higher variation compared to Model 1, as demonstrated in Figure 4. Analyzing the box plot, Models 3 and 4 exhibited low variation, but had elevated MSE values when compared to the first two models.

However, it is evident that all models achieved adequate temperature predictions, as shown in Figure 5, where the scatter plots demonstrate the close proximity of the predicted values to the actual values.

By analyzing the results, some hypotheses can be raised, such as the relationship between the number of neurons and hidden layers with the obtained results. It is observed that, in general, the increase in the number of hidden layers in Models 3 and 4, or performing a better search for the ideal number of nodes per layer in all models, could lead to more satisfactory results.

6. Conclusions

The results of MLPs generally met the expectations regarding temperature predictions and model performance, with Model 2 achieving the best outcome, even though it exhibited higher variation.

The hyperbolic tangent activation function, despite exhibiting greater variation, demonstrated better MSE compared to the sigmoidal function. This suggests that the hyperbolic tangent is more suitable for this type of study.

For future studies, alternative validation approaches can be considered to enhance network performance, such as employing K-fold cross validation, which can possibly help assess model reliability by validating the model on multiple subsets of data and reducing the risk of overfitting. Additionally, other types of ANNs can be explored, such as recurrent neural networks (RNNs) or extreme learning machines (ELMs), which could further improve the accuracy and performance of predictions for the specific problem at hand.

7. References

Brugnera, R. R., Mateus, R., Rossignolo, J. A., Chvatal, K. M. S., 2019. Open plan offices: the impact of different façade solutions on energy efficiency (in Portuguese), Ambiente Construído, Porto Alegre, Vol. 19, n. 3, p. 295-315, jul./set. 2019.

Bordoloi, N., Sharma, A., Nautiyal, H., Goel, V., 2018. An intense review on the latest advancements of Earth Air Heat Exchangers, Renewable and Sustainable Energy Reviews, Vol. 89, p. 261-280.

Haykin, S., 2009. *Neural Networks and Learning Machines*. 3rd edition. Pearson Education, Bengaluru, India.

Hollmuller, P.; Lachal, B., 2014. Air-soil heat exchangers for heating and cooling of buildings: Design guidelines, potentials and constraints, system integration and global energy balance. Applied Energy, Vol. 119, p. 476-487.

Kingma, D. P., Ba, J., 2014. Adam: A method for stochastic optimization. arXiv preprint arXiv:1412.6980v9.

Kumar, R., Kaushik, S. C., & Garg, S. N., 2006. Heating and cooling potential of an earth-to-air heat exchanger using artificial neural network. Renewable Energy, Vol. 31, Issue 8, pp. 1139–1155.

Marcondes, M. P., Mueller, C. M., Brandão, R. S., Shimomura, A. R. P., Brunelli, G., Leme, G. S. B. P., Gonçalves, J. C. S., Duarte, D. H. S., Frota, A. B., 2010. Comfort and thermal performance in the buildings of the new Petrobras research center in Rio de Janeiro (in Portuguese), Ambiente Construído, Porto Alegre, Vol. 10, n. 1, p. 7-29, jan./mar. 2010.

Ramírez-Dávila, L., Xamán, J., Arce, J., Álvarez, G., Hernández-Pérez, I., 2014. Numerical study of earth-to-air heat exchanger for three different climates, Energy and Buildings, Vol. 76, p. 238-248.

Rodrigues, M. K, Coswig, F. S., Camargo, K. R., Brum, R. S., Rocha, L. A. O., Santos, J. E. D., Isoldi, L. A., 2017. Study of the thermal potential of a soil-air heat exchanger in two types of soils in the municipality of Rio Grande (RS) (in Portuguese). Revista Brasileira de Energias Renováveis, Vol. 6, n. 3.

Romero-Méndez, R., Lara-Vázquez, P., Oviedo-Tolentino, F., Durán-García, H. M., Pérez-Gutiérrez, F. G., Pacheco-Vega, A., 2016. Use of Artificial Neural Networks for Prediction of the Convective Heat Transfer Coefficient in Evaporative Mini-Tubes. Ingeniería, Investigación y Tecnología, Vol. 17, Issue 1, pp. 23–34.

Silva, I. N., Spatti, D. H., Flauzino, R. A., 2010. *Artificial Neural Networks for Engineering and Applied Sciences (in Portuguese)*. Artliber Editora Ltda.

Siqueira, H., Macedo, M., Tadano, Y. de S., Alves, T. A., Stevan, S. L., Oliveira, D. S., Marinho, M. H. N., Neto, P. S. G. M., Oliveira, J. F. L., Luna, I., Filho, M. A. L., Sarubbo, L. A., Converti, A., 2020. Selection of Temporal Lags for Predicting Riverflow Series from Hydroelectric Plants Using Variable Selection Methods. Energies, 13(16), 4236.

Soni, S. K., Pandey, M., Bartaria, V. N., 2015. Ground coupled heat exchangers: A review and applications. Renewable and Sustainable Energy Reviews, Vol. 47, p. 83-92.

Tan, C. K., Ward, J., Wilcox, S. J., & Payne, R., 2009. Artificial neural network modeling of the thermal performance of a compact heat exchanger. Applied Thermal Engineering, Vol. 29, Issue 17-18, pp. 3609–3617.

8. Responsibility notice

The authors are the only responsible for the printed material included in this paper.